Journal of Alloys and Compounds 507 (2010) 502–507

Contents lists available at ScienceDirect

Journal of Alloys and Compounds

journal homepage: www.elsevier.com/locate/jallcom

Controlled shape of magnesium hydride synthesized by chemical vapor deposition

I. Matsumoto[a,*], T. Akiyama[b], Y. Nakamura[a], E. Akiba[a]

[a] Energy Technology Research Institute, AIST, 1-1-1 Higashi, Tsukuba, Ibaraki 305-8565, Japan
[b] Center for Advanced Research of Energy Conversion Materials, Hokkaido University, Kita 13 Nishi 8, Kita-ku, Sapporo, Hokkaido 060-8628, Japan

ARTICLE INFO

Article history:
Received 1 April 2010
Received in revised form 29 July 2010
Accepted 30 July 2010
Available online 7 August 2010

Keywords:
Hydrogen absorbing materials
Metal hydrides
Nanostructured materials
Vapor deposition
Scanning electron microscopy
X-ray diffraction

ABSTRACT

Three types of products were synthesized from Mg vapor and H_2 using chemical vapor deposition (CVD) at temperatures of 570–740 K and hydrogen pressures of 1–6 MPa. A CVD reactor with a moderate temperature gradient was developed, and the fluid behavior in the reactor was simulated to discuss the effects of temperature effects on product shape and phase accurately. The products were divided in terms of the temperature and hydrogen pressure at which they were synthesized. (1) At temperatures higher than or close to the formation equilibrium temperature of conventional MgH_2 powder at the hydrogen pressure applied, hexagonal particles of Mg were obtained. (2) When the temperature and hydrogen pressure were near equilibrium, curved fibers of Mg, MgH_2 or both were produced. (3) Straight fibers of MgH_2 were obtained at temperatures lower than the equilibrium temperature at the hydrogen pressure applied. Straight fibers of MgH_2 were directly synthesized from Mg vapor and H_2, while curved fibers were produced through hydrogen absorption by Mg fibers. These results indicate that MgH_2 can be synthesized in a uniform straight fibrous shape by controlling temperature and H_2 pressure during CVD.

1. Introduction

Magnesium hydride, MgH_2, has attracted great attention as a hydrogen storage material since its hydrogen capacity of 7.6 mass% stands out from known metal hydrides. However, the formation rate of MgH_2 is too low for practical applications [1]. As a matter of fact, Mg does not completely absorb hydrogen, and thus MgH_2 grains generally contain an unreacted Mg core [2]. In order to complete MgH_2 formation and to realize sufficient hydrogen storage capacity, previous studies have used additives and performed nanostructure fabrication to control material properties such as kinetics, thermodynamics and nanostructure in MgH_2 [3–11]. Although material design techniques have enabled certain improvements, hydrogen capacity inevitably decreases with as the amount of added substances and the oxidized surface area increase.

Instead of material design techniques, we applied process-engineering techniques to avoid the dominant rate-limiting steps of MgH_2 formation: hydrogen penetration into solid surfaces and hydrogen diffusion in the solid phase [12]. Surface contamination with magnesium oxide inhibits hydrogen penetration [13]. The hydride phase also plays a role in blocking hydrogen diffusion because hydrogen diffusion is extremely slow in hydrides [14]. In order to eliminate these problems, we developed a direct reaction process based on chemical vapor deposition (CVD). Using the CVD method, MgH_2 could be successfully produced from Mg vapor and H_2 [15] because H_2 can make contact with Mg without passing through the any of the solid phases. The MgH_2 synthesized by CVD consists of irregularly curved fibers and straight fibers of single crystals [15–18].

The CVD product of MgH_2 shows an equilibrium hydrogen pressure different from that of conventional MgH_2 powder: the hydrogen absorption of the CVD product reaches equilibrium at a temperature of 578 K and a hydrogen pressure of 1.3 MPa [16,17]; the equilibrium pressure of conventional MgH_2 powder is 0.2 MPa at the same temperature [19]. The nanostructure and strain in the materials have been reported to influence the thermodynamic properties of the Mg/H_2 system [20,21]. Further investigation of the relationship between the shape and hydrogen storage capacity of the fibers is strongly required to understand the phenomena. Therefore, we aim to prepare uniform MgH_2 particles in order to investigate the effects of particle shape. In this paper, we present the effect of CVD conditions, namely, temperature and pressure, on the shape of the product.

The CVD reactor used in our previous study had a steep temperature gradient in the boundary layer between the bulk gas and the substrate, on which the product of MgH_2 was synthesized [22].

* Corresponding author. Tel.: +81 29 861 4711; fax: +81 29 861 4711.
E-mail address: itoco.matsumoto@ni.aist.go.jp (I. Matsumoto).

0925-8388/$ – see front matter © 2010 Elsevier B.V. All rights reserved.
doi:10.1016/j.jallcom.2010.07.218

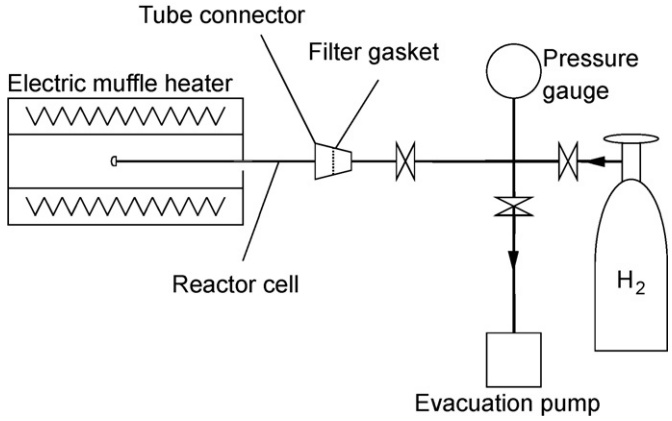

Fig. 1. Schematic of CVD reactor.

The temperature gradient produces the distribution of the product shape along the direction of product thickness. To evaluate the effect of temperature on product shape, a moderate temperature gradient is required. Therefore, we improved the reactor to have a more moderate temperature distribution than the previous one. In addition, the thermofluid behavior in the reactor was simulated to evaluate the temperature distribution in the reactor. MgH_2 was synthesized using the modified CVD reactor, and the temperature dependence and pressure dependence of product shape were evaluated considering the simulated temperature.

2. Experimental and simulation

2.1. CVD and analysis of MgH_2

The schematic drawing of the CVD apparatus is shown in Fig. 1. The apparatus consisted of an electric muffle furnace and a reactor tube made of stainless steel. The outer diameter of the reactor was 1/2 inch (1.27 cm) and the thickness of the reactor wall was 1.5 mm. The temperatures of the inner and outer walls of the reactor were measured prior to the experiments and are shown in Fig. 2. The measured temperature of the inner wall of the reactor was used for the boundary condition in the simulation. This temperature was not measured during CVD because thermocouples disturb the convection flow in the reactor. The temperature of the outer wall was monitored during CVD to determine whether the temperature gradient along the reactor agreed with the gradient shown in Fig. 2.

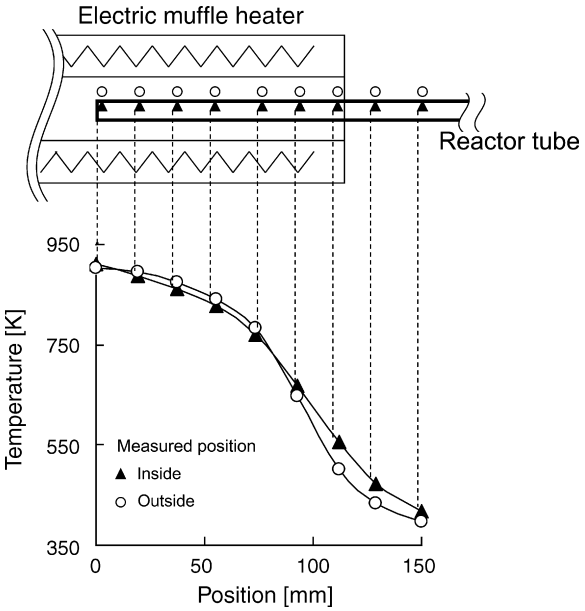

Fig. 2. Temperature difference between inside and outside wall.

At the closed end of the reactor, 1.7 g of Mg (99.9%, Kojundo Chemical Laboratory Co. Ltd.) was placed. The other end was attached to a gas line. The reactor was evacuated using a rotary pump, and then was filled with hydrogen gas (99.99999%). After repeating this procedure three times, the atmosphere inside of the reactor was filled with hydrogen. Hydrogen pressure was set at 1, 2, 4 or 6 MPa. The part of the reactor where Mg was placed was heated at 900 K for 60–200 h. During heating, the internal pressure was monitored, and kept constant. A few hours later, the reactor was naturally cooled down in an electric muffle furnace, detached from the gas line, and transferred into a glove box filled with purified Ar. The reactor was closed using a valve while it was off-line, thus the product was never exposed to air. The reactor was sliced into rings using a tube cutter in the glove box. The deposited CVD product was separated from the ring. Samples for characterization were set in sample holders for X-ray diffraction (XRD) analysis and field emission scanning electron microscopy (FE-SEM). The sample holder for XRD analysis was covered with plastic foil to prevent oxidization during the measurements. The FE-SEM sample was transferred in a sealed container, exposed to air in front of the machine, and set in an FE-SEM system within 10 s.

2.2. Thermofluid simulation of the CVD reactor

The fluid behavior and temperature distribution inside of the reactor was simulated using the thermofluid simulation software FLUENT (ANSYS Inc.). The simulation model was constructed on the basis of the actual reactor used in the CVD. It was assumed that 1 mL of Mg metal was heated at 900 K in the reactor filled with H_2 of 1, 2, 4 and 6 MPa. The boundary condition of inner wall temperature was fixed to the experimentally measured values shown in Fig. 2. At first, steady state of hydrogen convection was calculated under the assumption that Mg did not evaporate. This result was regarded as the initial condition at $t = 0$ s (t, time after starting the reaction). Then, the unsteady state simulation was started. Mg was assumed to evaporate at 900 K at a rate of 2×10^{-8} g/s. The evaporation rate was determined from the experimentally obtained amount of the CVD product per reaction time. The simulation model was regarded as a system closed at the filter gasket because the hydrogen flow through the filter was negligible in comparison with the flow in the simulated space.

Gaseous components composed of H_2 and Mg were treated as ideal gases. The properties of hydrogen were derived from the FLUENT database. A few properties of magnesium vapor, such as thermal conductivity and heat capacity, were derived from HSC Chemistry (Outotec Oyj). The viscosity of Mg vapor has not been reported to the best of our knowledge; therefore, it was assumed to be the same as that of hydrogen. The Mg vapor was assumed to consist only of monomers (single Mg atoms). The existence of Mg dimers (Mg diatomic molecules) [23] was not considered in this study because its equilibrium mole fraction in a mixture with monomers is negligible (less than 0.004%) [24]. To simplify the simulation model, neither the reaction between Mg and H_2 nor product deposition was not taken into account. The calculation was iterated until the standard deviation became less than 0.1%.

3. Results and discussion

3.1. Simulation results

The simulation results of the temperature distributions for $t = 0$ s and 10^4 s at hydrogen pressures of 1 and 6 MPa are shown in Fig. 3. The temperature distribution remained stationary from $t = 0$ s to 10^4 s. Even increasing the mole fraction of Mg vapor did not affect the temperature distribution over time. At pressures of both 1 and 6 MPa, the temperature distribution had a gentle gradient in the horizontal direction, that is, 10 K/mm at the maximum. At 6 MPa, the temperature contours in the range of temperatures from 400 to 800 K showed sigmoid curves, which produced a temperature difference of approximately 30 K between the gas bulk and the boundary layer on the reactor wall. The temperature gradient along the direction of product thickness was less than half of that in a previous study, in which the CVD reactor generated a temperature drop of 40 K within a range of 1 mm [22]. The temperature contours at 1 MPa ran in the vertical direction, and there was only a slight temperature gradient between the upper part and lower part of the reactor. At 2 and 4 MPa, the temperature gradients along the direction of product thickness were between those at 1 and 6 MPa. These results confirmed that the reaction setup realized moderate temperature gradient in the reactor as we intended. The temperature at which the product was synthesized was determined by reading the simulated temperature at the position where the product was obtained.

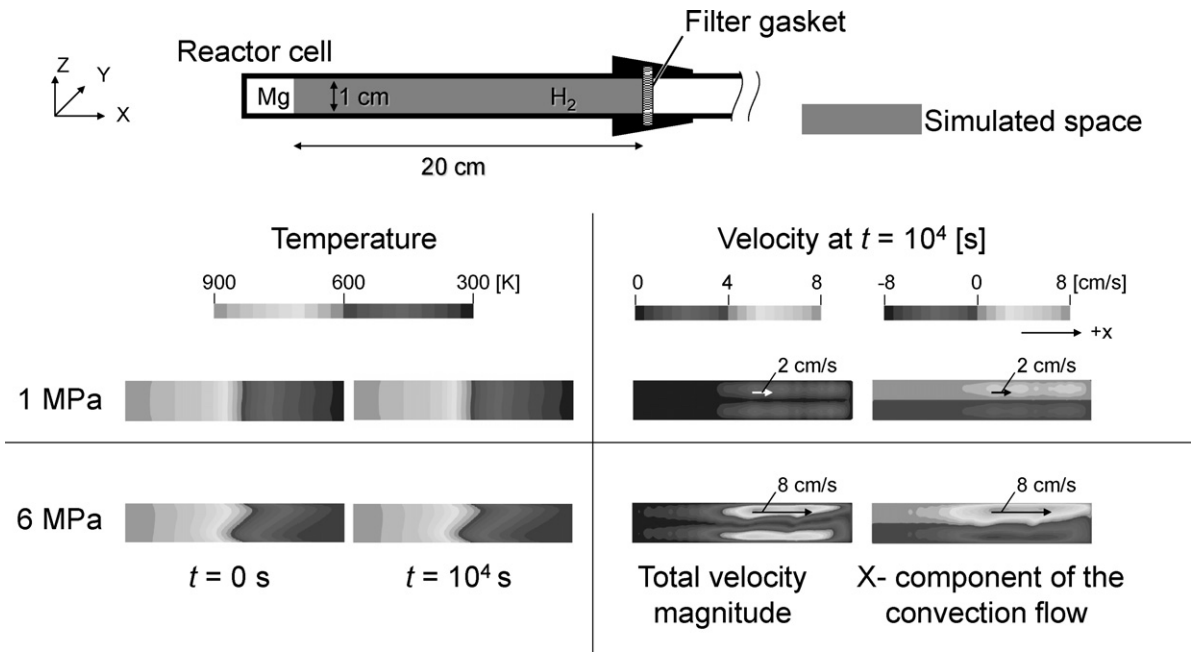

Fig. 3. Simulated temperature distribution and velocity of convection flow in the reactor.

The simulation results of the total velocity magnitude and the *x*-component of the convection flow are shown in Fig. 3. Such parameters did not change over time; thus only those at $t = 10^4$ s are listed. At each pressure simulated, the flow was rightward (from the high-temperature side to the low-temperature side) in the upper half of the reactor and leftward (from the low-temperature side to the high-temperature side) in the lower half. In the middle of the reactor, the total velocity and *x*-component showed the same magnitude. The convection flow was composed of the *x*-component. This means that the rightward flow in the upper half of the reactor and the leftward flow in the lower half did not run into each other. This result is crucial to understanding the experimental results below.

3.2. CVD of MgH_2

As a result of the CVD, the deposition was obtained in the entire pressure range studied. Products were formed on the reactor wall in the upper part, but not in the lower part. The simulation result indicated that the product was not obtained in the lower part because the Mg vapor was transferred from the higher temperature area to the lower temperature area by convection flow and deposited on the wall in the upper part. Thus, no Mg vapor remained or was deposited in the reflux in the lower part of the reactor.

The products differed in appearance depending on the position where they were obtained. In the higher temperature area, plate-shaped powders with metallic luster were obtained. The product in the lower temperature area was white powder, showing neither visible luster nor reflection. The white powder was easily removed from the wall, while the metallic powder was difficult to remove. The boundary between the white powder and the metallic powder could be clearly observed. The temperatures at the boundary during CVD are listed in Table 1 with the formation equilibrium temperatures of MgH_2 for conventional Mg powder [19] at each of the H_2 pressures applied during the CVD. The boundary temperature and equilibrium temperature were similarly dependent on hydrogen pressure, although each boundary temperature was lower than the equilibrium temperature at the corresponding pressure.

Table 1
Formation equilibrium temperatures of conventional MgH_2 powder and temperatures at the boundary between metallic powder and white powder.

Pressure [MPa]	Equilibrium temperature[a] [K]	Boundary temperature [K]
1	642	630
2	675	640
4	712	700
6	736	710

[a] Obtained by substituting the values of ΔH^0 and ΔS^0 reported in Ref. [15] into van't Hoff's equation: $\ln P_{H_2} = \Delta H^0/RT - \Delta S^0/R$, where P_{H_2} is the equilibrium H_2 pressure, R is the gas constant, T is the equilibrium temperature, ΔH^0 is the standard enthalpy of formation (−74.5 kJ/mol-H_2), and ΔS^0 is the standard entropy of formation (−135.2 J/K mol-H_2).

3.3. Characterization of the product synthesized by CVD

The XRD patterns of the products are shown in Fig. 4. At 1, 2 and 4 MPa of H_2, the products of white powders synthesized at tem-

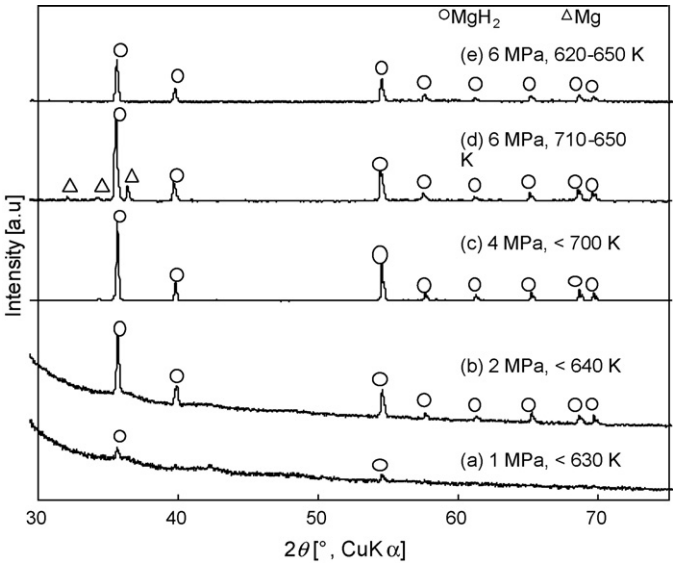

Fig. 4. XRD patterns of CVD products.

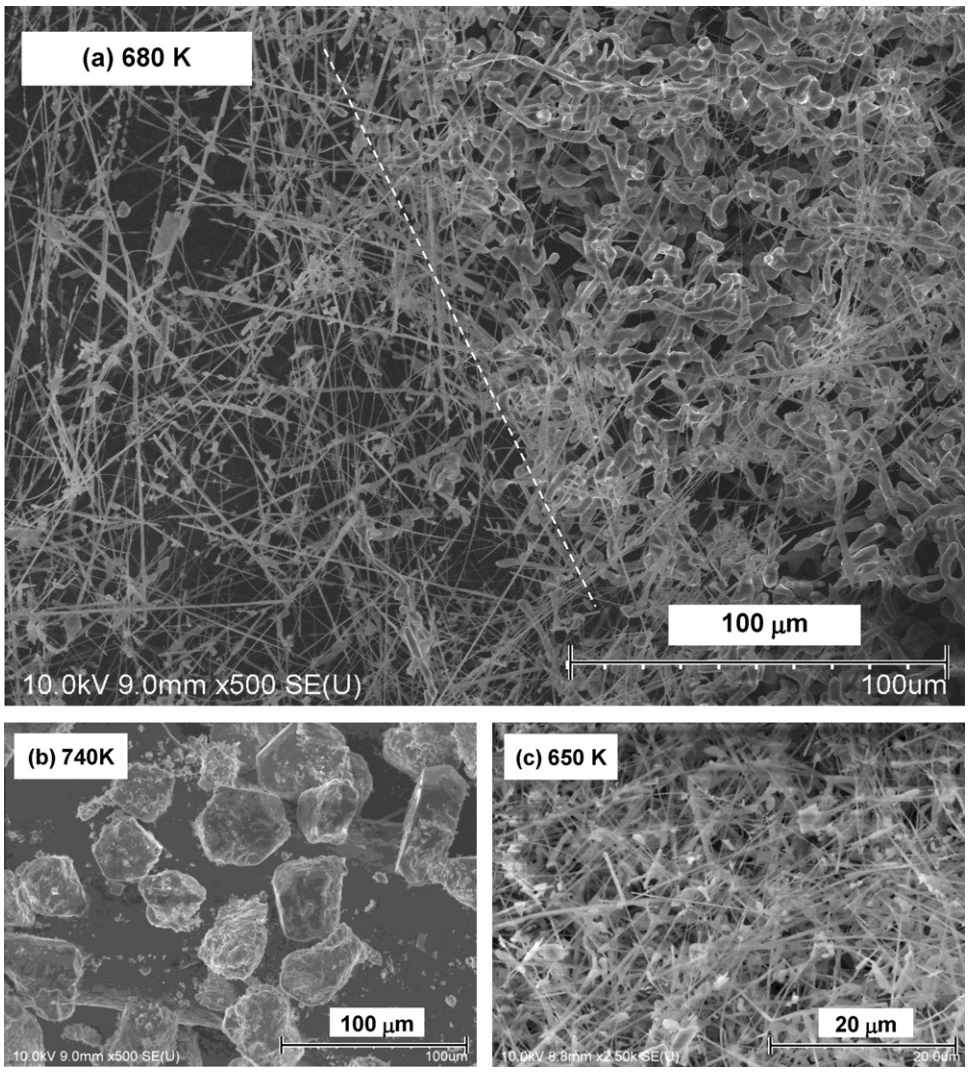

Fig. 5. SEM images of CVD products synthesized at 6 MPa.

peratures lower than the boundary listed in Table 1 were all MgH_2 (Fig. 4a–c). The product obtained at the H_2 pressure of 6 MPa and at temperature between 710 and 650 K contained a small fraction of Mg (Fig. 4d) even though it was a white powder. The white powder obtained at lower temperatures, for example, less than 650 K, was MgH_2 as shown in Fig. 4e.

FE-SEM images of the products are shown in Figs. 5 and 6. The products shown in Figs. 5b, 6a, d and g were obtained at temperatures higher than the boundary listed in Table 1. They contained hexagonal particles and plates with 120° corners showing a hexagonal crystal habit. This indicates that the products are all Mg metal.

FE-SEM images of the white products synthesized at temperatures lower than the boundary are shown in Figs. 5c, 6c, f and i. The white products consisted of straight fibers and were determined to be MgH_2 by XRD analysis. The straight fibers of MgH_2 were successfully synthesized separately from the curved fibers.

The curved fibers shown in Fig. 5a (right side) and Fig. 6b, e and h existed between the boundary listed in Table 1 and the area where straight fibers were obtained. In Fig. 5, the curved fibers are shown on the right (Fig. 5a), while the straight fibers are shown on the left. There was a clear boundary between the curved and straight fibers, as indicated by the white dashed line in the FE-SEM image, although the boundary was not visible to the naked eye. The lower temperature side was at the left of the boundary. The product obtained at low-temperatures was determined to be a mixture of Mg and MgH_2 by XRD analysis (Fig. 4d); however, the phase of the curved fibers could not be determined between the two phases. Li et al. reported helpful information for discussing the phase and growth mechanism of the curved fiber. They prepared various nanostructured Mg samples using a vapor deposition technique in an inert atmosphere by changing the deposition conditions [7]. The shape of the curved fibers (which they call “nanowires”) of Mg that they prepared is similar to the shape of the curved fibers in this study. Judging from their shape, the curved fibers obtained in this study are likely related to the Mg wires reported by Li et al. A Mg wire absorbs hydrogen at levels as high as 7.6 mass% within 30 min at 573 K [7]. In our previous study, the CVD product was identified as MgH_2, even though it contained curved fibers [16,17]. These two reports suggested that curved Mg fibers absorb H_2 and form curved MgH_2 fibers during CVD depending on the experimental conditions. Here, a fraction of the curved fibers did not complete hydrogen absorption, and therefore unreacted Mg was found, as shown in Fig. 4d. The straight fibers of MgH_2 were likely synthesized through the direct reaction between Mg vapor and hydrogen rather than through the hydrogenation of Mg fibers. The difference in fiber curvature was due to the difference in MgH_2 formation route.

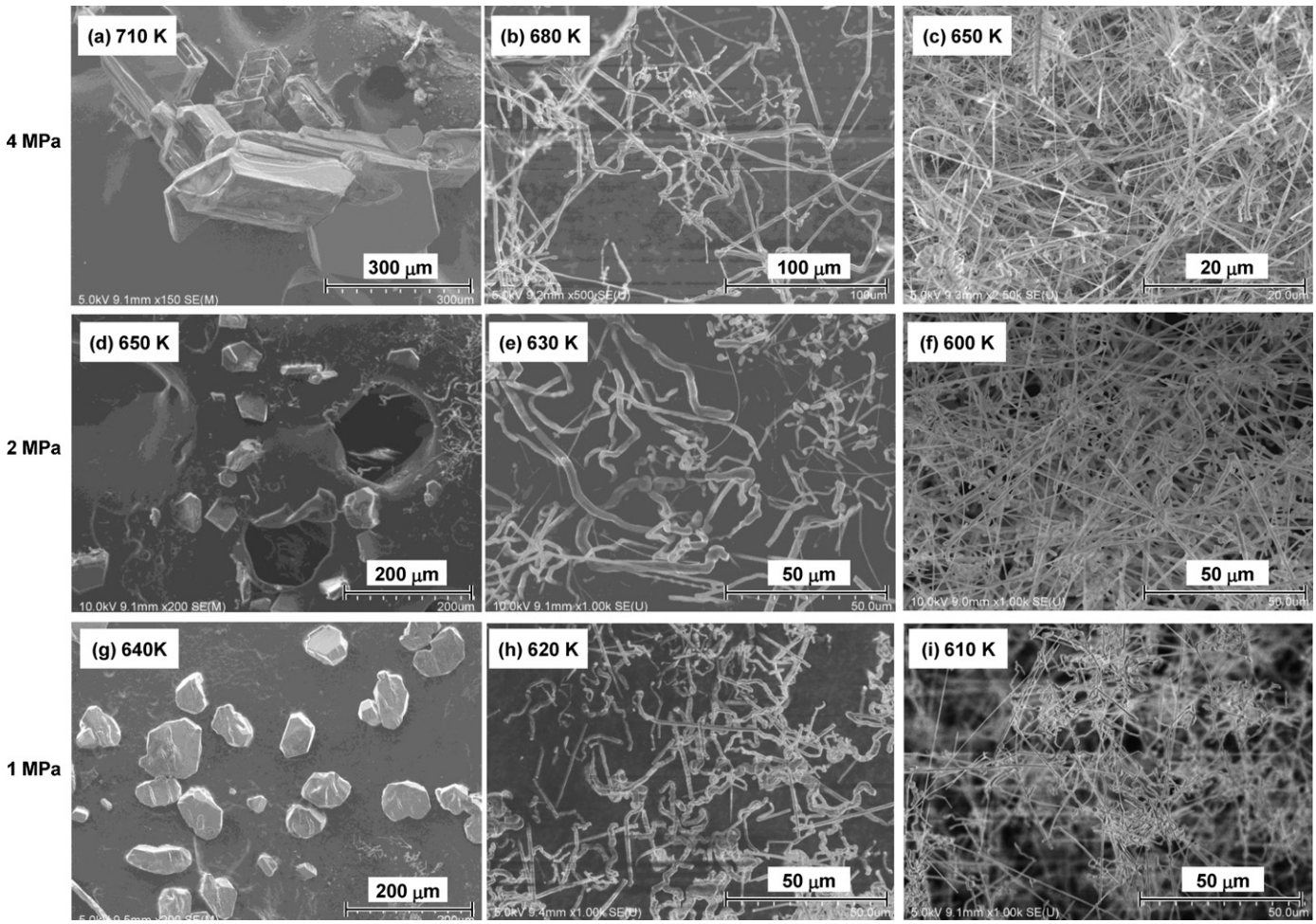

Fig. 6. SEM images of CVD products synthesized at 1, 2 and 4 MPa.

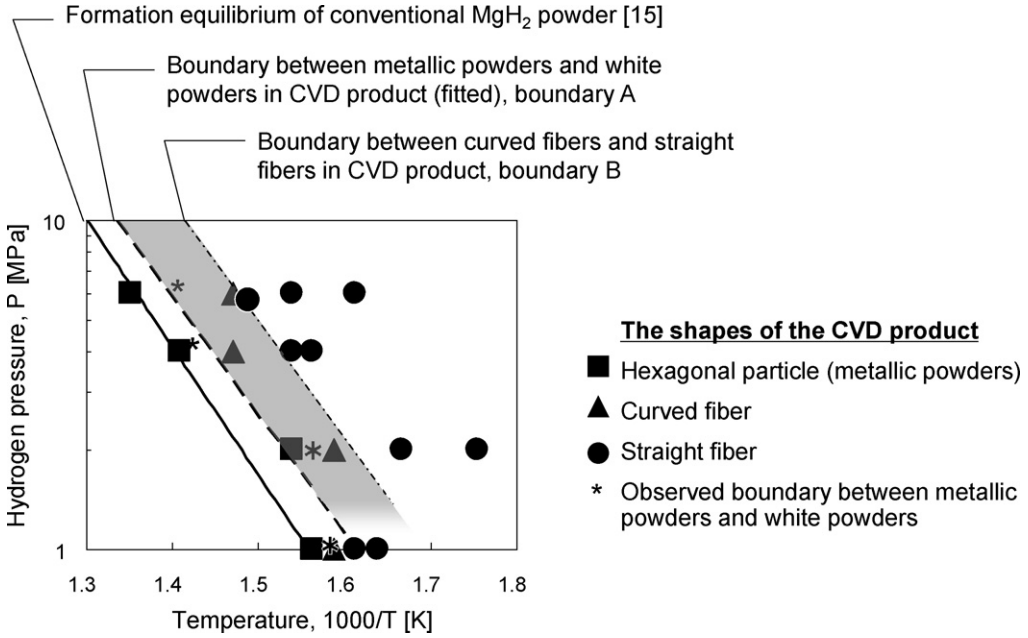

Fig. 7. Pressure–temperature diagram of CVD product.

The diameters of the straight MgH_2 fiber and the curved fibers were apparently different: the diameter of the straight fibers was approximately 0.5 μm and that of the curved fibers was approximately 2–3 μm under all CVD conditions studied. The difference in fiber diameter is due to the different in growth mechanisms of the straight MgH_2 and the curved Mg fibers.

3.4. Pressure–temperature diagram of the CVD products

The shape and phase of the products synthesized by CVD in this study are plotted in the pressure–temperature diagram shown in Fig. 7. The solid line indicates the equilibrium condition for MgH_2 formation with conventional Mg powders [19]. The observed boundary (boundary A) between metallic powders and white powders in the product is also plotted and fitted with a dashed line. The boundary between the curved and straight fibers (boundary B) is shown as the dash-dotted line. The pressure–temperature diagram was divided by the two boundary lines into three parts. (1) At temperatures higher than boundary A, Mg powder particles of hexagonal plate shape were obtained. (2) Curved fibers of Mg and/or MgH_2 were obtained at the temperatures between the two boundaries (gray area). (3) Straight fibers of MgH_2 were obtained in the region at temperatures lower than boundary B.

The region of metallic Mg particle formation extended to an area with temperatures lower than the equilibrium temperature of MgH_2 formation for conventional Mg powder (solid line) [19]. This means that the Mg particles were not involved in the equilibrium of MgH_2 formation between Mg metal and hydrogen gas during the CVD process.

The product synthesized at temperatures lower than the boundary B consisted of straight fibers of MgH_2. At 1 MPa, both the curved and straight fibers coexisted at the temperature higher than the dash-dotted line. The boundary between the two types of fibers did not fit the dash-dotted line. As shown in the simulation results, when the pressure was decreased, the convection flow became slower. The slower convection flow resulted in a longer resident time in the high-temperature area, and enabled MgH_2 formation at temperatures higher than the dash-dotted line. Conversely, the convection flow at pressures higher than 2 MPa was so rapid that it carried Mg vapor to the low-temperature area before MgH_2 formation reached completion.

4. Conclusions

The effects of temperature and pressure during CVD, by which MgH_2 was produced from Mg vapor and hydrogen, on product shape were examined. In order to discuss the effect of temperature precisely, a CVD reactor with a moderate temperature gradient was developed and the thermofluid behavior in the reactor was simulated. The shape and phase of CVD products were dependent on the temperature and pressure at which the products were synthesized. We obtained three types of products divided by two boundaries. (1) Mg particles were obtained at temperatures higher than or close to the equilibrium temperature of MgH_2 formation for conventional Mg powder. (2) Curved fibers of Mg and/or MgH_2 were obtained at the temperature and H_2 pressure between the two boundaries. (3) Straight fibers of MgH_2 were obtained separately from both the curved fibers and the Mg particles at temperatures lower than the MgH_2 formation equilibrium temperature. The straight fibers were product of the direct deposition of MgH_2, while the curved fibers were eventual product of Mg fiber deposition and the subsequent hydrogenation. This study demonstrated that uniform straight fibers of MgH_2 can be synthesized using the CVD method.

Acknowledgements

This work was supported in part by the New Energy and Industrial Technology Development Organization (NEDO) under "Advanced Fundamental Research on Hydrogen Storage Materials (Hydro-Star)". The simulation was conducted using the High-Performance Computing System in Hokkaido University, Japan. The FE-SEM work was conducted at the AIST Nano-Processing Facility, supported by the "Nanotechnology Network Japan" of the Ministry of Education, Culture, Sports, Science and Technology (MEXT), Japan.

References

[1] L. Schlapbach, A. Zuttel, Nature 414 (2001) 353–358.
[2] L. Belkbir, E. Joly, N. Gerard, Int. J. Hydrogen Energy 6 (1981) 285–294.
[3] J. Huot, G. Liang, S. Boily, A.V. Neste, R. Schulz, J. Alloys Compd. 293–295 (1999) 495–500.
[4] J.L. Bobet, C. Even, Y. Nakamura, E. Akiba, B. Darriet, J. Alloys Compd. 298 (2000) 279–284.
[5] G. Barkhordarian, T. Klassen, R. Bormann, Scripta Mater. 49 (2003) 213–217.
[6] B. Sakintuna, F. Lamari-Darkrim, M. Hirscher, Int. J. Hydrogen Energy 32 (2007) 1121–1140.
[7] W.Y. Li, C.S. Li, H. Ma, J. Chen, J. Am. Chem. Soc. 129 (2007) 6710–6711.
[8] G. Barkhordarian, T. Klassen, R. Bormann, J. Alloys Compd. 364 (2004) 242–246.
[9] C. Zlotea, M. Sahlberg, S. Ozbilen, P. Moretto, Y. Andersson, Acta Mater. 56 (2008) 2421–2428.
[10] M. Danaie, D. Mitlin, J. Alloys Compd. 476 (2009) 590–598.
[11] N. Hanada, T. Ichikawa, H. Fujii, J. Alloys Compd. 446–447 (2007) 67–71.
[12] N. Gerard, S. Ono, in: L. Schlapbach (Ed.), Topics in Applied Physics, vol. 67, Springer-Verlag, Berlin, Heidelberg, 1992, pp. 178–180 (Chapter 4).
[13] A. Andreasen, T. Vegge, A.S. Pedersen, J. Phys. Chem. B 109 (2005) 3340–3344.
[14] G. Friedlmeier, M. Groll, J. Alloys Compd. 253–254 (1997) 550–555.
[15] I. Saita, T. Toshima, S. Tanda, T. Akiyama, Mater. Trans. 47 (2006) 931–934.
[16] I. Saita, T. Toshima, S. Tanda, T. Akiyama, J. Alloys Compd. 446–447 (2007) 80 L 83;
I. Saita, T. Toshima, S. Tanda, T. Akiyama, J. Alloys Compd. 482 (2009) 556.
[17] I. Saita, T. Toshima, S. Tanda, T. Akiyama, J. Alloys Compd. 482 (2009) 556.
[18] I. Saita, T. Akiyama, MRS Proceedings 2006 Fall, 2006, 971E, 0971-Z08-10.
[19] J.F. Stampfer Jr., C.E. Holley Jr., L.F. Stuttle, J. Am. Chem. Soc. 82 (1960) 3504–3508.
[20] R.A. Varin, T. Czujko, Ch. Chiu, Z. Wronski, J. Alloys Compd. 424 (2006) 356–364.
[21] A. Baldi, M. Gonzalez-Silveira, V. Palmisano, B. Dam, R. Griessen, Phys. Rev. Lett. 102 (2009) 226102.
[22] I. Saita, T. Akiyama, E. Akiba, 2007 MRS Fall Meeting, 2007 (Abstract S4.5).
[23] W.J. Balfour, A.E. Douglas, Can. J. Phys. 48 (1970) 901–914.
[24] Z. Slanina, Thermochim. Acta 207 (1992) 9–13.